Available online at www.sciencedirect.com
SCIENCE DIRECT
Polymer 46 (2005) 10618–10625
polymer
www.elsevier.com/locate/polymer

Kinetic limitation in the formation of end-linked elastomer networks

B. Meissner*, L. Matějka

Institute of Macromolecular Chemistry of the Academy of Sciences of the Czech Republic, Heyrovský Sq. 2, 162 06 Prague 6, Czech Republic

Received 23 May 2005; received in revised form 1 September 2005; accepted 9 September 2005
Available online 29 September 2005

Abstract

The effects of the initial ratio r of the concentrations of functional groups contained in the crosslinker and polymer precursor, on the extent of an end-linking reaction at constant reaction time were calculated analytically on the basis of the second-order reaction kinetics. The result of a recent Monte Carlo simulation (Gilra et al. 2000) which supplied discrete data at a constant number of MC steps is shown to be essentially identical with the kinetics-based calculation. Using the analytical approach and the theory of branching processes, theoretical dependence of sol fraction, w_S, on r at constant reaction time was calculated and shown to satisfactorily describe the experimental data measured on two series of poly(tetrahydrofuran) networks (Takahashi et al. 1995, thiol-allyl end-linking reaction, molar mass of precursor $M_A = 2.5$ and 4.4 kg/mol). In the series based on longer chains, rather high values of r_{opt} (i.e. r for minimal w_S) were found which cannot be accounted for by mere kinetic limitations. A second factor, tentatively ascribed to a partial loss, for end-linking, of functional groups of one component (side reactions; steric hindrance leading to incomplete reaction) was found to give, together with the kinetic limitation effect, a satisfactory description of the w_S–r data in general. The hydrosilylation PDMS networks based on vinyl-terminated polysiloxanes behave in a similar manner with the kinetic effect being of minor importance.

Keywords: End-linked elastomer networks; Effects of stoichiometry; Kinetic limitations

1. Introduction

Model elastomer networks have often been synthesized by end-linking precursor chains terminated by reactive groups A with star-shaped crosslinker molecules containing three or more reactive groups B, using an addition reaction A + B = A − B. According to the predictions of the theory of branching processes TBP [1,2], an ideal model network with a maximal modulus, G, and a zero sol fraction, w_S, is formed, in the absence of side-reactions if the initial ratio $r = B/A$ of the concentrations of crosslinker-to-precursor functional groups and the final extent of reaction, $\alpha_A = \alpha_B$, are both unity. Unbalanced stoichiometry, $r \neq 1$, and/or incomplete conversion of the minority functional groups are predicted to lead to network imperfections resulting in a decreased modulus and a non-zero increasing sol fraction.

A number of experimental studies (e.g. Refs. [3–9]) have shown that in a series of end-linked networks differing in r, the maximal modulus and minimal sol fraction are not obtained at the theoretically expected value $r = 1$, but at an optimal ratio, r_{opt}, higher than unity. The phenomenon was observed for hydrosilylation-end-linked networks (–Si–H + CH_2=CH– ⇒ –Si–CH_2–CH_2–) based on vinyl-terminated [3–6] and hydrogen-terminated [7] polysiloxanes, for networks based on hydroxyl-terminated polysiloxanes end-linked with tetraethoxysilane [8] and also for networks based on diallyl-terminated poly(tetrahydrofuran) (PTHF) polymer precursor end-linked with tetrathiol crosslinker using a thiol-ene reaction [9] (–S–H + CH_2=CH– ⇒ –S–CH_2–CH_2–). In case of hydrosilylation networks based on vinyl-terminated precursors, the observed effect was shown to be due to a partial loss of SiH groups contained in volatile species formed by a disproportionation side reaction of the silane crosslinker [3]; steric hindrance resulting in an unequal reactivity of the reactive sites of the crosslinker has also been proposed as a possible explanation [4].

Recently, the formation of end-linked polymer networks with a range of precursor polymer chain lengths and crosslink concentrations has been studied by Gilra et al. using Monte Carlo simulations [10]. In a given network series with the initial ratio r ranging from 0.9 to 1.6, the network properties were evaluated and compared at the same (high) number of Monte Carlo steps per repeat unit (n_{MCS}) in order to model the experimental condition of equal time of cure. It was shown that under such isochronous cure conditions the optimum r values

* Corresponding author. Tel.: +42 296 809 384; fax: +42 296 809 410.
E-mail address: meissner@imc.cas.cz (B. Meissner).

0032-3861/$ - see front matter © 2005 Elsevier Ltd. All rights reserved.
doi:10.1016/j.polymer.2005.09.036

are non-stoichiometric; for the longest 50-mer precursor studied, r_{opt} was around 1.2. This effect appears to be the result of the kinetic limitation that prevents systems at near-stoichiometric conditions ($r \approx 1$) from achieving high extents of reaction in a reasonable cure time (i.e. at a reasonable n_{MCS}).

In the present paper the problem of kinetic limitations is addressed using an analytical approach based on the second-order rate equation. Its results are compared with the Monte Carlo predictions [10] and with experimental data obtained on the off-stoichiometry systems. For this purpose, sol fraction measurements on allyl-thiol end-linked poly(tetrahydrofuran) networks [9] and on hydrosilylation-end-linked poly(dimethylsiloxane) networks were used, and predictions of the theory of branching processes [1,4] utilized.

2. Calculated dependence of the extent of reaction on the ratio *r* and on the reaction time

2.1. Second-order kinetics

Let us assume that the kinetics of an end-linking process based on alternating copolymerization of the polymer precursor and crosslinker components is dominated by the time scale of the reaction time, i.e. the reaction time is much larger than the diffusion time. Here we are interested in the rate of decrease in the concentration of functional groups since such information is required for theoretical calculation of the sol fraction and other network properties in systems where a full extent of reaction has not been achieved. The relevant rate equation for the kinetics of the reaction A+B=A−B is assumed to be of the second order. Its integrated form reads

$$kt = \frac{1}{A-B}\ln\frac{B(A-x)}{A(B-x)}$$

k is the rate constant, A and B, are the initial molar concentrations of A and B functional groups and x is the concentration of reacted functional groups at time t.

In the region of $r=(B/A)<1$, the functional groups B of the crosslinker are the minority groups and the extent of reaction—the degree of conversion α_m of the minority groups—is equal to the degree of conversion of groups B: $\alpha_B = x/B$. Thus, for $r<1$:

$$\alpha_m = \frac{1-E_1}{r-E_1}, \quad \text{where } E_1 = \exp\left[\frac{Bkt(1-r)}{r}\right] \tag{1a}$$

For $r>1$, the functional groups A of the polymer are the minority groups and the extent of reaction $\alpha_m = \alpha_A = x/A$ is given by

$$\alpha_m = \frac{r(1-E_2)}{1-rE_2}, \quad \text{where } E_2 = \exp[Akt(r-1)] \tag{1b}$$

In the stoichiometric case ($r=1$), $Akt=Bkt$, $\alpha_m=\alpha_A=\alpha_B$ and

$$\alpha_m = \frac{Akt}{1+Akt} \tag{1c}$$

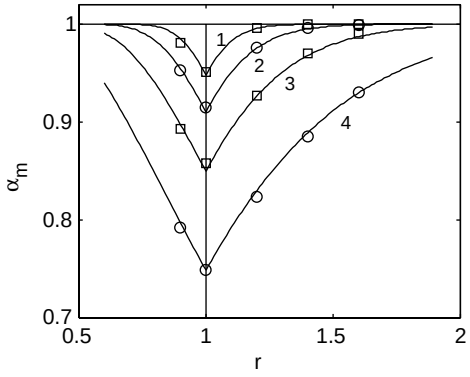

Fig. 1. Dependence of the degree of conversion of minority groups, α_m, on the ratio r. Curves are based on the second-order kinetics, Eqs. (1a)–(1c). Points: MC simulation. The $Akt(Bkt)/n_{MCS} \times 10^{-4}$ values: 1, 18.14/40; 2, 10.15/10; 3, 5.65/3; 4, 2.98/1.

Fig. 1 shows the dependences of α_m on r (curves) calculated from Eqs. (1a)–(1c) using four different constant values of the dimensionless time Bkt (for $r<1$)=Akt (for $r>1$): 18.14, 10.15, 5.65, 2.98. In each case, at $r=1$, a minimum degree of conversion is attained, the value of which is determined by Eq. (1c). With increasing stoichiometric imbalance, the conversion of minority groups increases and tends to approach unity.

For the system of a bifunctional precursor, tetrafunctional crosslinker (molar mass $M_B=0.5$ kg/mol), for a full conversion of minority groups and four different molar masses M_A of the precursor, the theory of branching processes TBP (Appendix A) predicts the dependence of sol fraction on r given in Fig. 2. In the region of $r>1$ and with M_A increasing from low values up to 9 kg/mol, the sol fraction w_S at a given r tends to decrease. For M_A higher than ca. 9 kg/mol (and also at $r<1$ for all values of M_A), the w_S–r dependence is almost independent of the precursor molar mass M_A.

With the knowledge of the dependence of α_m on r at a constant reaction time (Eqs. (1a)–(1c)) and utilizing the results of the theory of branching processes (Appendix A, dependence of sol fraction on α_m and r), one can construct a graph showing dependences of w_S on r at different (constant) reaction times (Fig. 3). The following parameter values were used: the

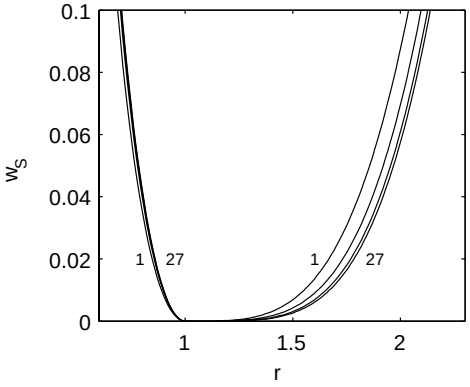

Fig. 2. Dependence of sol fraction on r at full conversion of minority groups; calculated from TBP. Values of M_A (kg/mol) are 1, 3, 9, 27.

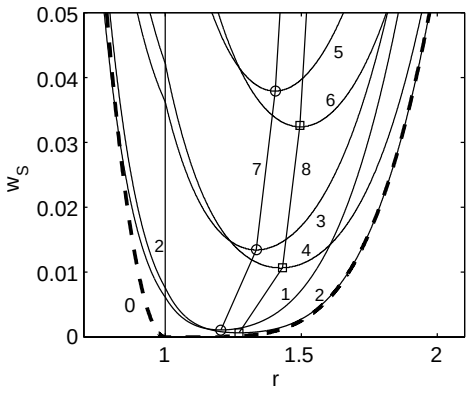

Fig. 3. Curve 0: Dependence of w_S on r for $\alpha_m=1$, $M_A=50$ kg/mol. Curves 1–6: dependences of w_S at constant $Akt(Bkt)$ on r for parameter values given below.

Curve	1	2	3	4	5	6
M_A (kg/mol)	1	50	1	50	1	50
$Akt(Bkt)$	11	11	4.8	4.8	3.4	3.4

Lines 7 and 8: correlation between the minimal sol fraction $w_{S,min}$ and the corresponding stoichiometric ratio r_{opt}; line 7, $M_A=1$ kg/mol; line 8, $M_A=50$ kg/mol.

crosslinker (pentaerythritol tetrakis(3-sulfanylpropanoate)) molar mass $M_B=0.544$ kg/mol, its functionality $f_B=4$, the functionality of the precursor $f_A=2$; the values of the remaining parameters are given in the caption to Fig. 3. Curves calculated for isochronous cure conditions with very large $Akt(Bkt)\gtrsim 100$ are practically identical with that calculated for $\alpha_m=1$ (curve 0); the shape of the curves is unsymmetrical with a mimimum at $r=1$. For smaller $Akt(Bkt)$ values, the minimum at $r=1$ disappears and the w_S–r dependence assumes a shape of an almost symmetrical valley with a minimal sol fraction $w_{S,min}$ at stoichiometric ratio $r=r_{opt}>1$. For $Akt(Bkt)=11$ and a short precursor (curve 1), $r_{opt}\approx 1.20$ and $w_{S,min}\approx 0.1\%$. For longer precursor chains, r_{opt} increases but for M_A higher than ca. 10 kg/mol it levels off, reaching some 1.27 (curve 2). Thus, the effect of M_A on w_S seen in Fig. 2 tends to persist even in the case of a constant reaction time, i.e. when the conversion of minority groups is a function of r and at $r=1$ has a minimal value (Fig. 1). With decreasing reaction time, the r_{opt} values tend to increase slowly both for short and long precursor chains while $w_{S,min}$ values increase steadily.

Summarizing, the analysis based on a combination of second-order kinetics with equations of the theory of branching processes predicts that the kinetic limitation effect should be responsible for values of r_{opt} as high as 1.5 or even higher provided they are accompanied by sol fractions $w_{S,min}$ at least 3.5% or higher. If $w_{S,min}$ is low then r_{opt} is predicted to be low as well.

2.2. Monte Carlo results

The details of the Gilra et al. simulation procedure are described in Ref. [10]. In their Fig. 2, the authors present, for the network based on a 50-mer precursor, the resulting dependences of the fraction of unreacted chain ends, z, on the number, n_{MCS}, of Monte Carlo steps per repeat unit for five different ratios r: 0.9, 1, 1.2, 1.4, and 1.6. The number of Monte Carlo steps can be considered to be proportional to the reaction time. From Fig. 2 in Ref. [10], we have read off values of z for five values of r at the following constant values of $n_{MCS}\times 10^{-4}$: 1, 3, 10, 40. For $r\geq 1$, $\alpha_m=\alpha_A=(1-z)$ while for $r=0.9$, $\alpha_m=\alpha_B=(1-z)/0.9$. In Fig. 1, the Monte Carlo dependence of the conversion α_m of the minority groups on the ratio r is plotted for the four constant values of *MCSRU* (points). Each dependence shows a minimum of conversion at the stoichiometric condition $r=1$ and an increase in conversion with increasing excess of any of the two functional groups. The Monte Carlo simulation results are seen to be identical with the result of the analytical solution (Eqs. (1a)–(1c)); the values of $Akt(Bkt)$ were adjusted to obtain a fit of the curves to the MC points. The exact correspondence between the Monte Carlo simulation and the second-order-kinetics calculation of the α_m–r dependence, which is seen in Fig. 1, is due to the condition of constant time and/or constant n_{MCS}. On the other hand, the MC simulation yields a slower increase in α_m with $\log(n_{MCS})$ than is the increase in α_m with log time as obtained by the second-order-kinetics calculation (Table 1).

Table 1
Times and MC steps to reach a given conversion

α_m at $r=1$	n_{MCS}	$n_{MCS,rel}$	Akt	Akt_{rel}
0.75	1×10^4	1	3	1
0.85	3×10^4	3	5.65	1.9
0.91	10×10^4	10	10.15	3.4
0.95	40×10^4	40	18.14	6

At $r=1$, an increase in α_m from 0.75 to 0.95 requires a six-fold increase in the time of the second-order process. In the MC simulation on a 50-mer network, n_{MCS} must be increased forty times. The factor is chain-length-dependent and from the result of a Monte Carlo simulation on a 20-mer network (Trautenberg et al., Fig. 1 in Ref. [11]), one can estimate the corresponding required $n_{MCS,rel}$ to be 22.

3. Comparison with experimental data

3.1. PTHF thiol-ene networks

Jong and Stein prepared a set of stoichiometric thiol-ene networks based on precursor chains of diallyl-terminated poly(tetrahydrofuran) end-linked with a tetrafunctional thiol (pentaerythritol tetrakis(3-sulfanylpropanoate)); the prepolymer molar masses M_A ranged from 2 to 13.6 kg/mol [12]. The first stage of end-linking was carried out in benzene solution at 60 °C to prevent phase separation of crosslinker and precursor and, thus, to ensure the homogeneity of the network. During a period of 20–30 min, all crosslinker molecules are assumed to have reacted with at least one prepolymer chain and the solvent could then be removed. The main part of the reaction and the determining stages of network build-up took then place in dry state under nitrogen at 88 °C for 2 days, i.e. under the condition of a constant reaction time. The obtained degree of conversion was subsequently conserved by cooling the product down to

Table 2
Characteristics of the PTHF networks prepared by Takahashi et al. [9]

Code	M_A (kg/mol)	f_A	r_{opt}	$w_{S,min}$ (%)
U025	2.54	1.85	1.29	3.1
U044	4.36	2.0	1.37	1.2
U052	5.19	1.94	1.57	4.6
U079	7.91	1.94	1.60	5.54
U102	10.2	2.09	2.37	10.4

room temperature. The measured values of w_S ranged from 0.6 to 3.4% with an average of ca. 2% and the preparation method was considered as adequately reproducible.

Using the experimental procedure of Jong and Stein, Takahashi et al. prepared five series of networks based on prepolymers with molar masses ranging from 2.54 to 10.2 kg/mol and with wide ranges of r in each series [9]. From their sol fraction data for each series (given in Fig. 3 in Ref. [9]), we have determined the respective values of $w_{S,min}$ and r_{opt} (Table 2).

For the U025 and U044 series, the $w_{S,min}$ values lie in the same low region as found by Jong and Stein and the w_S–r data can be considered suitable for an experimental test of the kinetic limitation concept. The experimental dependence of w_s on the ratio r of the U025 series is re-plotted here in Fig. 4, that of the U044 series in Fig. 5. In the same graphs, theoretical sol fraction dependences on r are drawn for several constant values of α_m including unity. The curves were calculated using the results of the theory of branching processes [1] in the form quoted by Patel et al. [4] (Appendix A). Precursor polymers with number-average functionalities $f_A < 2$ (Table 2) were assumed to consist of a mixture of bifunctional and monofunctional chains, their mass fractions being given by $(f_A - 1)$ and $(2 - f_A)$, respectively.

From comparison of the experimental points with the TBP curves, one can obtain estimates of the degree of conversion of the minority groups, attained in experiments. For example, in Fig. 5, the network with a near-stoichiometric value of $r = 0.94$ has a high sol fraction of 0.1 because of its low degree of conversion: the point lies on the theoretical curve calculated for $\alpha_m = \alpha_B = 0.8$. A minimal value (0.012) of the experimental sol fraction was obtained with $r = 1.37$; the point lies on the curve calculated for a much higher conversion of $\alpha_m = \alpha_A = 0.95$. With still increasing excess of crosslinker groups, the reaction of the minority vinyl groups becomes practically complete, approaching unity for $r > 1.8$. The degree of conversion, α_m, achieved in the individual networks after a 2-day cure at 88 °C can be estimated from Figs. 4 and 5 or calculated from the experimental w_S–r data using the theoretical equations given in Appendix A. The values of α_m obtained by the latter method are plotted vs r in Fig. 6 and are fitted by the curves drawn according to Eqs. (1a)–(1c) with suitably adjusted values of $Akt(Bkt)$, which are given in Table 3. The fit of the curves to the points may be regarded as satisfactory.

Assuming now that the r-dependence of α_m in the U025 and U044 series is given by Eqs. (1a)–(1c) with the respective values of $Akt(Bkt)$, one can calculate the corresponding dependences of w_S on r. They are drawn in Figs. 4 and 5 as thick lines fitting the experimental dependences with a reasonable accuracy. Thus, kinetic limitation can be viewed

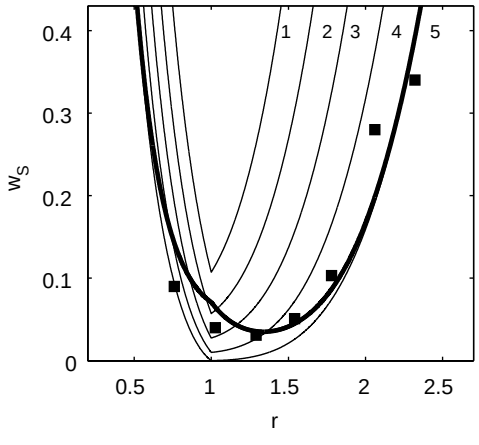

Fig. 4. Dependence of sol fraction on r for the network series U025. Points: experimental [9]. Thin lines are drawn for constant values of α_m: 1, 0.8; 2, 0.85; 3, 0.9; 4, 0.95; 5, 1.0 (equations given in Appendix A, parameter values in Table 2). Thick line is drawn for α_m dependent on r according to Eqs. (1a)–(1c) with $Akt(Bkt)$ given in Table 3.

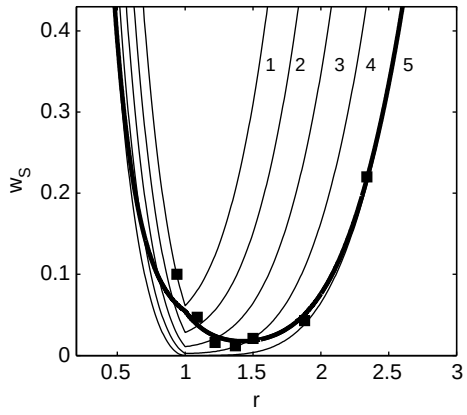

Fig. 5. Dependence of sol fraction on r for the network series U044. For legend see Fig. 4.

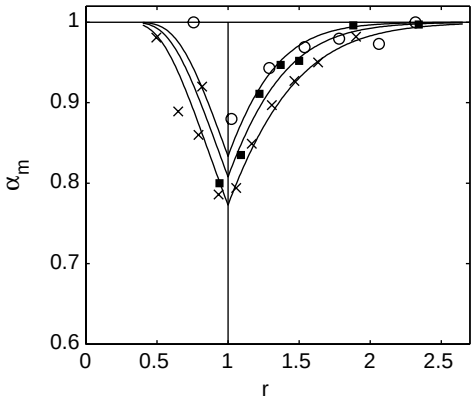

Fig. 6. Dependence of the extent of reaction α_m on the ratio r for the U025, U044, U052 series. Points: estimates based on experimental sol fractions and TBP; (○), U025; (■), U044; (×), U052. Curves are drawn according to Eqs. (1a)–(1c) with the values of $Akt(Bkt)$ given in Table 3.

Table 3
Parameter values of the PTHF network series

Code	M_A (kg/mol)	f_{emp}	$Akt(Bkt)$
U025	2.54	1	5.0
U044	4.36	1	4.2
U052	5.19	1.20	3.4
U079	7.91	1.16	2.8
U102	10.2	1.45	2.1

f_{emp}, empirical factor obtained from a shift of w_S data into the region expected by the TBP (see below).

upon as the only factor governing the sol fraction and r_{opt} values of the U025 and U044 series.

The remaining three network series of Takahashi et al. show a more complicated behavior. This is shown in Fig. 7 where the sol fraction data for the U052 network series are plotted vs the nominal stoichiometric ratio (open circles). (Hereinafter, the nominal stoichiometric ratio will be denoted by r_0). Unlike the U025 and U044 networks in Figs. 4 and 5, the sol fraction points of the U052 networks obtained at a high excess of crosslinker groups lie outside the theoretically expected range of nominal ratio r_0. A similar type of behavior is observed with the series U079 and U102 (graphs not shown here). It appears that apart from the kinetic limitation effect, some other factor must play a role here.

An inspection of Fig. 7 offers a tentative explanation: a certain fraction of crosslinker groups is ineffective and does not take part in the end-linking reaction. An effective stoichiometric ratio, r, can then be assumed to govern the end-linking reaction, with r being lower than the nominal ratio, r_0, by an empirical factor f_{emp} higher than unity and independent of r_0:

$$r = \frac{r_0}{f_{emp}}$$

In Fig. 7, the sol fraction data are plotted once more, this time vs the effective ratio r (full squares). The value of the empirical parameter f_{emp} (=1.2) was obtained by suitable

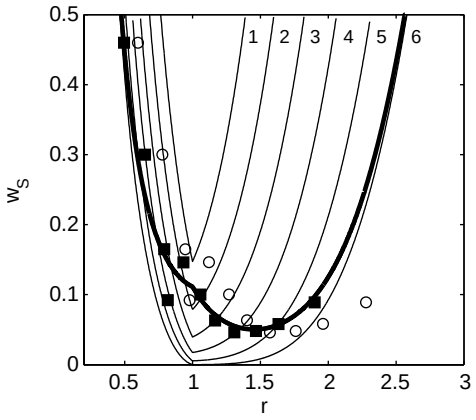

Fig. 7. Dependence of sol fraction on r for network series U052. Points: experimental. Open circles are plotted vs the nominal ratio r_0; full squares plotted vs the effective ratio $r=r_0/1.2$. Thin lines are drawn according to the theoretical equations given in Appendix A for parameter values given in Table 2 and with α_m: 1, 0.75; 2, 0.8; 3, 0.85; 4, 0.9; 5, 0.95; 6, 1.0. Thick line: α_m dependent on r according to Eqs. (1a)–(1c) with $Akt(Bkt)$ in Table 3.

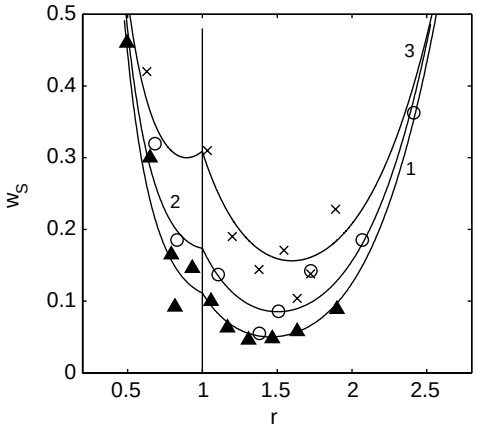

Fig. 8. Dependence of sol fraction on the effective ratio r. Points: experimental; (▲), U052; (○), U079; (×), U102. Lines are drawn according to the theoretical equations given in Appendix A for parameter values given in Table 2 and with α_m dependent on r according to Eqs. (1a)–(1c) with $Akt(Bkt)$ values given in Table 3.

adjustment to make the points move into the theoretically expected region. The α_m values were then determined from w_S and the (effective) ratios r in the same manner as before; the α_m–r data (Fig. 6) and w_S–r data (Fig. 7) were processed in the same way as described above. The thick line in Fig. 7 is drawn through the w_S–r points with α_m dependent on r according to Eqs. (1a)–(1c) and with $Akt(Bkt)$ given in Table 3. The fit of the curve to the points is satisfactorily good and supports the assumption of f_{emp} being independent of r_0.

The sol fraction data on the U079 and U102 series were processed in the same way as those on the U052 series and the obtained parameters f_{emp}, $Akt(Bkt)$ are also given in Table 3. The dependence of w_S on the effective stoichiometric ratio r is plotted in Fig. 8 for the U052, U079 and U102 series together with the respective lines calculated for the r-dependent conversions. The graph shows the net effect of the kinetic limitation after the contribution of the second factor characterized by f_{emp} has been empirically filtered off by substituting r for r_0. With increasing M_A, the concentration of functional groups decreases and, accordingly, $Akt(Bkt)$ decreases as well (Table 3). This is seen in Fig. 8 to lead to a gradual increase in $w_{S,min}$, r_{opt}, in agreement with the predictions shown in Fig. 3.

As mentioned above, the sol fractions measured by Jong and Stein on their stoichiometric PTHF networks are almost independent of M_A and do not exceed some 3.5%. These findings are rather different from those of Takahashi et al. (cf. Table 2). One of the possible reasons for this seeming controversy may be a difference in the rate of the end-linking reaction obtained in the two studies; unequal reaction rates may have resulted from possible differences in the experimental reaction conditions, raw materials, efficiency of the catalyst, etc. A significantly higher rate constant k would lead to high $Akt(Bkt)$ values which would make $w_{S,min}$ smaller, r_{opt} closer to unity and the effect of M_A in the 2–13 kg/mol range less significant; this is in line with the findings in Ref. [12].

Jong and Stein carried out a model reaction with

stoichiometric amounts of monofunctional compounds (allyl phenyl ether and methyl 3-sulfanylpropanoate) in a benzene solution, under conditions similar to those used for network preparation. After the reaction, benzene and unreacted reaction components were evaporated and the remaining thiol-ene reaction product analyzed. Its NMR spectrum showed the presence of two possible structures of the product and the authors concluded that 'no significant side reactions are observable' [12]. However, they did not analyze the volatile part of the reaction mixture, which might have contained volatile products of a possible side reaction. The analysis of Jong and Stein shows the presence of the expected product but does not exclude the presence of side reactions. A tentative explanation for f_{emp} can assume the incomplete reaction of the crosslinker groups due to steric hindrance [4] and/or their loss in side reactions.

3.2. Hydrosilylation networks of PDMS

Patel et al. published equilibrium swelling data on networks obtained in a wide range of nominal stoichiometric ratio, r_0, using a tetrafunctional silane crosslinker and vinyl-terminated poly(dimethylsiloxane) (PDMS) precursors with molar masses 10.3, 18.5 and 53.5 kg/mol, respectively [4]. The experimental dependence of the polymer volume fraction in the swollen network at equilibrium, v_2, on the nominal ratio, r_0, is characterized by a pronounced maximum at a nominal stoichiometric ratio, r_{opt}, which for the three series attains values around 1.6, 1.55 and 1.65, respectively, without any notable trend with increasing M_A. So far, no attempt has been made to interpret the phenomenon of $r_{opt} > 1$ observed with hydrosilylation networks on the basis of the kinetic limitation concept. As mentioned above, another factor was shown to be responsible for it: a disproportionation reaction of the silane crosslinker which results in a partial loss of Si–H groups through volatilization of low-molar-mass products of the side reaction [3]. Only the remaining Si–H groups take part in network formation and determine the effective stoichiometric ratio r.

To investigate the phenomenon, we have prepared a series of non-stoichiometric hydrosilylation networks based on a vinyl-terminated poly(dimethylsiloxane) ($M_A = 49.5$ kg/mol) and measured their sol fractions; the experimental details are given in Appendix B. The obtained dependence of w_S on the nominal ratio r_0 (crosses) has a minimum around 1.55 (Fig. 9). The data are plotted once more in the same graph vs the effective ratio $r = r_0/f_{emp}$ (full squares). The value of the empirical parameter $f_{emp} = 1.53$ was adjusted to make the points move into the region demarcated by the theoretical curve drawn for $\alpha_m = 1$.

The dependence of w_S on the effective ratio r has a minimum at $r \approx 1$ and, in this respect, it differs from the behavior of the thiol-ene networks whose effective r for a minimal sol is distinctly higher than unity (Figs. 7, 8). In Fig. 10, the dependence of w_S on the effective r is compared, for the hydrosilylation networks, with the kinetic-limitation-based predictions; the curves 1 and 2 are drawn using the TBP and Eqs. (1a)–(1c) with two Akt(Bkt) values, 12 and 5,

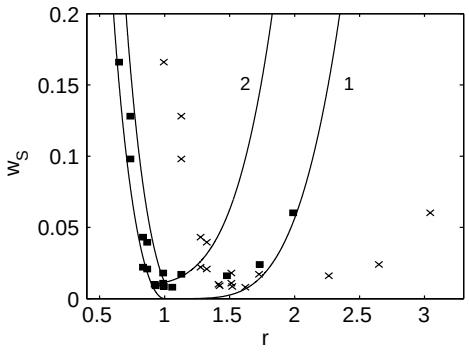

Fig. 9. Dependence of w_S on r for the hydrosilylation network series ($M_A = 49.5$ kg/mol). Points: experimental; crosses, plotted vs nominal ratio r_0; full squares, plotted vs effective ratio r. Curves drawn according to the TBP, 1, $\alpha_m = 1$; 2, $\alpha_m = 0.9$.

respectively. Systematic deviations can be seen in both cases and the fit of the curves to the data is rather of a qualitative character. However, a conclusion is perhaps justified that in hydrosilylation networks based on vinyl-terminated polymers the contribution of the kinetic effect is not pronounced, most probably due to a high rate of reaction (high k, Akt) and seems to be greatly overshadowed by the second factor which is characterized by the value of f_{emp}. For our hydrosilylation networks, the difference $(f_{emp} - 1)$ is obviously related to the loss of crosslinker groups in the side reaction [3] with a possible contribution of steric hindrance [4]. For the thiol-ene networks such interpretation of the observed $f_{emp} > 1$ phenomenon is tentative only and no independent evidence can be offered.

In a recent paper, Lai et al. have found that in a series of hydrosilylation networks based on a SiH-terminated PDMS end-linked with a triallyloxy crosslinker, the nominal vinyl/silane ratio r_0 required for a maximal modulus is 1.4 [7]. They concluded that kinetic effects may play the major role here because if loss of SiH groups due to side reactions was mainly responsible, then the ratio r_{opt} should be expected to be lower than or close to unity. We have made some preliminary experiments on end-linking a SiH-terminated PDMS ($M_A =$

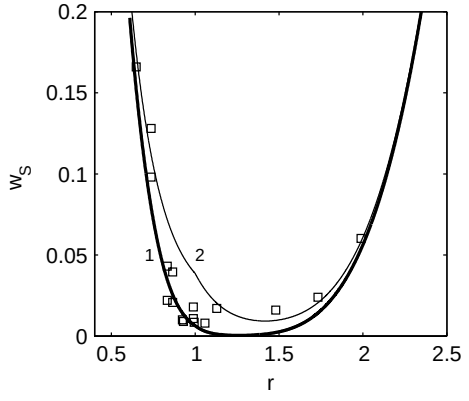

Fig. 10. Dependence of w_S on r for the hydrosilylation network series ($M_A = 49.5$ kg/mol). Experimental points are plotted vs the effective ratio r. Curves 1 and 2 are drawn using the Eqs. (1a)–(1c) with Akt(Bkt) values 12 and 5, respectively.

28 kg/mol) with a tetravinyl crosslinker (H-networks) and have found features different from those of the current hydrosilylation networks based on vinyl-terminated PDMS (Vi-networks). With Vi-networks, the maximum in modulus is pronounced while with H-networks it was rather flat in the range of nominal r_0 from 0.9 to 1.4. The maximal modulus was by some 30% lower than that in the Vi-network series based on a polymer precursor with the same M_A. In the region of $r_0<1$, the modulus of H-networks decreases rather slowly with decreasing r_0 and a rough estimate of the critical ratio for gelation, $r_{0,g}$, has a small value, lower than ca. 0.2. (For Vi-networks, an estimate of $r_{0,g}$ tends to be higher than 0.5; the theoretical $r_{0,g}$ is equal to 1/3 if $f_A=2, f_B=4, \alpha_m=1$.) Some of the observations can be given a straithforward explanation. If some of the silane groups are lost for end-linking of the H-networks, then from definition the nominal ratio r_0 (=Vi/SiH) should be lower than the effective r and the critical ratio for gelation, $r_{0,g}$, in the $r_0<1$ region is thus shifted to a lower value than is the theoretical one (while in the Vi-networks, r_0=SiH/Vi is shifted to a value higher than is the theoretical, or, the effective one). The disproportionation reaction wherein two SiH-terminated precursor chains take part produces one volatile bifunctional molecule and one longer silane-terminated chain. This leads to a decrease in the concentration of precursor chains and, consequently, to a decrease in the concentration of elastically active network chains and in the value of the attainable modulus. In our experiment, the observed r_{opt} was slightly higher than unity ($\approx 1.2\pm0.1$) and possible factors responsible for the shift of r_{opt} to a higher value can be both the kinetic effect and the incomplete reaction of vinyl crosslinker groups due to steric hindrance.

The off-stoichiometry effects in hydrosilylation networks will be the subject of our forthcoming study.

4. Conclusions

The effects of the stoichiometric imbalance on the extent of an alternating end-linking copolymerization were calculated analytically on the basis of the second-order reaction kinetics. At a constant reaction time, the degree of conversion of minority groups, α_m, is predicted to have a minimum at $r_0=1$ and, with increasing stoichiometric imbalance, to increase and approach unity; α_m is a function of a dimensionless parameter $Akt(Bkt)$ proportional to the reaction time t and rate constant k. The magnitude of the kinetic limitation effect increases with a decrease in $Akt(Bkt)$.

The result of a Monte Carlo simulation (Gilra et al. 2000), which supplied discrete data at a constant number of MC steps is shown to be essentially identical with the kinetics-based calculation.

Experimental w_S–r_0 measurements and the reasons for $r_{opt}>1$ were analyzed using the predictions of the kinetic limitation concept and the equations of the branching theory. Apart from the kinetic effect, a second factor was found to be generally operative. It manifests itself by some of the w_S–r_0 points falling outside the TBP expected range and can be filtered off by plotting the w_S data vs the effective ratio $r=r_0/f_{emp}$, where the empirical factor f_{emp} is found by a suitable adjustment. Its difference from unity can be interpreted quite generally as being due to an incomplete utilization, for end-linking, of the functional groups of one of the reaction components. Such reasoning implies that functional groups can be lost due both to side reactions and to steric hindrance leading to incomplete reaction of all the functional groups on the cross-links.

The kinetic limitation effect appears to be the sole factor for the U025 and U044 PTHF network series. For the remaining three PTHF series, both the kinetic effect and the second factor ascribed tentatively to the loss of crosslinker groups for end-linking are significant. The Vi-networks show a qualitatively similar behavior but the kinetic effect seems to be of minor importance and evidence was published for the loss of crosslinker silane groups in a side reaction. The behavior of H-networks is rather complex and requires a deeper study. In principle, three factors may be involved: loss of silane precursor groups due to a side reaction, incomplete reaction of vinyl crosslinker groups due to steric hindrance and the kinetic effect. The first factor would shift r_{opt} to a lower value, the second and third factor to a higher value.

Sivasailam and Cohen report data on the r-dependence of equilibrium swelling of the Vi-networks prepared in the absence or presence of an unreactive diluent. The r_{opt} value ($\sim$1.45) was found to change only negligibly for different precursor preparation concentrations of the same precursors [5]. This result suggests that the kinetic limitation effect is insensitive to the precursor concentration in the course of end-linking.

Acknowledgements

The authors are greatly indebted to the Grant Agency of the Czech Republic for financial support of this work within the grant project No. 203/05/2252.

Appendix A

The initial reactant mixture contains A_1^0, A_2^0 mol of mono- and two-functional polymer and B_4^0 mol of four-functional crosslinker; a_2 is the mole fraction of the reactive groups on two-functional polymer molecules in their mixture with monofunctional ones,

$$a_2=\frac{2A_2^0}{A_1^0+2A_2^0}=\frac{2(f_A-1)}{f_A}$$

f_A is the number-average functionality of the precursor polymer, w_{A1}, w_{A2} and w_{B4} are the mass fractions of mono- and two-functional polymers and of four-functional crosslinker, respectively; α is the extent of reaction (degree of conversion) of crosslinker groups B. In the Miller–Macosko theory of branching processes [1], expressions are derived, which are quoted by Patel et al. [4] in the form:

$$U = r\alpha\left[\left(\frac{4-3r\alpha^2a_2}{4r\alpha^2a_2}\right)^{0.5} - 0.5\right]^3 + 1 - r\alpha$$

$$V = \left(\frac{4-3r\alpha^2a_2}{4r\alpha^2a_2}\right)^{0.5} - 0.5$$

and the mass fraction, w_S, of soluble material is given by

$$w_s = w_{A2}U^2 + w_{A1}U + w_{B4}V^4$$

Appendix B

Materials. The vinyl-terminated poly(dimethylsiloxane) precursor DMS V35, and the crosslinker tetrakis(dimethylsilyloxy)silane (SIT7278.0, purity 97%) were supplied by the ABCR Company. The catalyst, the platinum–divinyltetramethyldisiloxane complex in xylene is the product of Aldrich Comp. The characteristics of the precursor given by the producer are the following: concentration of vinyl groups [Vi] = 0.0438 ± 0.007 mol/kg, M_A = 49.5 kg/mol (in reasonable agreement with 2/[Vi] = 46 ± 8 kg/mol).

Preparation of networks was done in the manner described in the literature [13]. The concentration, [H], of SiH groups in the crosslinker was calculated from its theoretical molar mass and purity ([H] = 0.97 × 4/0.328 = 11.83 mol/kg). For the concentration of vinyl groups in the precursor, the average value, [Vi], given above was taken. The crosslinker and the polymeric precursor were mixed in the required molar ratios, r_0, of SiH to vinyl groups; some 10–15 mixtures were prepared with values of r_0 ranging from ca. 0.8 to 3. The Pt-catalyst diluted with xylene was added (~20 ppm of Pt) and the mixture thoroughly agitated and degassed. The end-linking reaction was carried out in a Teflon mould for 3 days at 70 °C.

Extraction of networks. Thin specimens (150–200 mg, ca. 1 mm thick) were cut from the networks and subjected to a static extraction with toluene for at least 5 days; the solvent was replaced twice a day. The mass of the unextracted (m_1) and extracted dry specimen (m_2) was determined and used to calculate the mass-fraction of extractables, $E = (m_1 - m_2)/m_1$. The commercially made PDMS reactants used in several studies were found to contain 2–5% unreactive impurities of low molar mass (0.3–1.5 kg/mol). Following the method of Meyers et al. [14] and Gottlieb et al. [15], we used GPC measurements on the unreacted vinyl-terminated precursor and on several network extracts to determine the mass fractions, E_{ur}, of low-molar-mass unreactive species. The averaged value of E_{ur} obtained for the DMS V35 precursor was 0.037. The mass-fractions of sol, w_S, were then obtained by correcting the mass fraction of the toluene extract for the presence of unreactive species: $w_S = (E - E_{ur})/(1 - E_{ur})$.

References

[1] Miller DR, Macosko CW. Macromolecules 1976;9:206–11.
[2] Dušek K. Adv Polym Sci 1986;78:1–59.
[3] Macosko CW, Saam JC. Polym Bull 1987;18:463–71.
[4] Patel SK, Malone S, Cohen C, Gillmor JR, Colby RH. Macromolecules 1992;25:5241–51.
[5] Sivasailam K, Cohen C. J Rheol 2000;44:897–915.
[6] Larsen AL, Hansen K, Sommer-Larsen P, Hassager O, Bach A, Ndoni S, et al. Macromolecules 2003;36:10063–70.
[7] Lai SK, Batra A, Cohen C. Polymer 2005;46:4204–11.
[8] Takeuchi H, Cohen C. J Chem Phys 2000;112:6910–6.
[9] Takahashi H, Shibyama M, Fujisawa H, Nomura S. Macromolecules 1995;28:8824–8.
[10] Gilra N, Cohen C, Panagiotopoulos AZ. J Chem Phys 2000;112:6910–6.
[11] Trautenberg HL, Sommer J-U, Göritz D. Macromol Symp 1994;81:153–60.
[12] Jong L, Stein RS. Macromolecules 1991;24:2323–9.
[13] Macosko CW, Benjamin GS. Pure Appl Chem 1981;53:1505–18.
[14] Meyers KO, Bye ML, Merril EW. Macromolecules 1980;13:1045–54.
[15] Gottlieb M, Macosko CW, Benjamin GS, Meyers KO, Merrill EW. Macromolecules 1981;14:1039–46.